A Methodology and Implementation of Automated Emissions Harmonization for Use in Integrated Assessment Models

Matthew J. Gidden[a,*], Shinichiro Fujimori[b], Maarten van den Berg[c], David Klein[d], Steven J. Smith[e], Detlef P. van Vuuren[c], Keywan Riahi[a]

[a] *International Institute for Applied Systems Analysis, Schlossplatz 1, A-2361 Laxenburg, Austria*
[b] *Center for Social and Environmental Systems Research, National Institute for Environmental Studies, 16-2 Onogawa, Tsukuba, Ibaraki 305-8506, Japan*
[c] *PBL Netherlands Environmental Assessment Agency, Postbus 30314, 2500 GH The Hague, Netherlands*
[d] *Potsdam Institute for Climate Impact Research (PIK), Member of the Leibniz Association, P.O. Box 60 12 03, D-14412 Potsdam, Germany*
[e] *Joint Global Change Research Institute, 5825 University Research Court, Suite 3500, College Park, MD 20740*

Abstract

Emissions harmonization refers to the process used to match greenhouse gas (GHG) and air pollutant results from Integrated Assessment Models (IAMs) against a common source of historical emissions. To date, harmonization has been performed separately by individual modeling teams. For the hand-over of emission data for the Shared Socioeconomic Pathways (SSPs) to climate model groups, a new automated approach based on commonly agreed upon algorithms was developed. This work describes the novel methodology for determining such harmonization methods and an open-source Python software library implementing the methodology. A case study is presented for two example scenarios (with and without climate policy cases) using the IAM MESSAGE-GLOBIOM that satisfactorily harmonize over 96% of the total emissions trajectories while having a negligible effect on key long-term climate indicators. This new capability enhances the comparability across different models, increases transparency and robustness of results, and allows other teams to easily participate in intercom-

*Corresponding author
Email address: gidden@iiasa.ac.at (Matthew J. Gidden)

parison exercises by using the same, openly available harmonization mechanism.

Keywords: Integrated Assessment Models, Harmonization, Greenhouse Gases (GHGs), Air Pollution

---

Software Availability

`aneris`, first made available in 2017, is available online at `https://github.com/iiasa/aneris` as a free and open-source Python software library (approximately 2000 lines of code). The `aneris` software was developed by the lead author whose contact information is shown on the title page of this manuscript. Documentation for the `aneris` Python package, including software requirements, is available online at `http://software.ene.iiasa.ac.at/aneris/`.

Introduction

Integrated Assessment Models (IAMs) are tools used to understand the complex interactions between energy, economy, land use, water, and climate systems. IAMs provide global projections of systemic change by dividing the world into a number of representative regions (typically 10 to 30), the definition of which is distinct for each model [1]. Results from IAMs are integral in a number of international studies, which notably include projections of climate and energy futures. Recently, the IAM community has developed scenarios based on the Shared Socioeconomic Pathways (SSPs) [2] which quantify a variety of potential global futures. The SSPs are designed to be used in research that include Earth System Model (ESM) simulations, climate impact, adaptation and climate mitigation studies [3, 4].

While IAMs are implemented in myriad ways[1], including simulation and optimization, the core inputs and outputs are similar across different models. Modeling teams incorporate data on energy systems, land use, economics, demographics and emissions sources and concentrations, among other data, in order to provide a consistent starting point for future projections. The models then provide estimates of future trajectories of these variables under various socioeconomic and technological assumptions as well as proposed policy constraints, e.g., targets for future Greenhouse Gas (GHG) emissions.

The emissions trajectories calculated by IAMs are critical inputs for ongoing, worldwide scientific community efforts in the Coupled Model Intercomparison Project (Phase 6) (CMIP6) [5], which is utilizing a number of marker SSP scenarios developed by the IAM community (Scenario Model Intercomparison Project (ScenarioMIP)[6], Aerosol Chemistry Model Intercomparison Project (AerChemMIP)[7], among others). These trajectories are endogenously calculated

[1]IAM models are numerous and have a long history in the scientific literature. Various IAMs have collaborated to produce community IAM documentation (available online: `http://themasites.pbl.nl/models/advance/index.php/ADVANCE_wiki`) which readers can access for a full treatment of model implementation and features.

by modeling the individual technologies and sectors that contribute towards the emissions of different air pollutants and GHGs as well as various mitigation technologies. However, the historical emissions starting points of models can differ by large amounts depending on the region, sector, and emissions species.

In practice, IAMs calculate the total source intensity of emitting technologies, for example the total activity of coal power plants in China, and incorporate emissions-intensity factors for individual gas species, for example the quantity of sulfur emissions from coal plants per megawatt-hour of production. Models are generally *calibrated* to historical data sources in one or more base years. Results in the historical period may differ between models as a result of the sometimes large uncertainties in historical data sets. Models can also differ in their choice of base-year, which may lag behind available inventory data. In addition, models have varying sectoral, regional, and fuel aggregations.

The global climate change community has recently developed a new global historical emissions data set for both anthropogenic emissions (i.e., the Community Emissions Data System (CEDS) [8] and open-burning Land-use and Land-use Change (LULUC) emissions [9]) which, in conjunction with the SSP IAM trajectories, will be used for climate-related modeling exercises of CMIP6.

When participating in intercomparison exercises in which a consistent historical starting point is required (e.g., in CMIP6), model teams incorporate a single, common historical data set through *harmonization*. Harmonization refers to the process of adjusting model results to match a selected historical time series such that the resulting future trajectories are consistent with the original modeled results and provide a smooth transition from the common historical data. In the emissions context, this means that each individual combination of model region, model sector, and emissions species must be harmonized. Depending on the total number of model regions, sectors, and emissions species, this can require the selection of thousands to tens-of-thousands of harmonization methods.

Harmonization has been addressed in previous studies as it is a common practice in the IAM and climate change communities. For example, [10] describes the use of scaling routines for the 5 regions used in the IPCC Special Report on

Emissions Scenarios (SRES) [11]; however, only total emissions were harmonized in the exercise, thus there is no sectoral dimension. Further, [12] describes the impacts of choosing various harmonization routines on future trajectories. During the evaluation of the Representative Concentration Pathways (RCPs), IAM results have been harmonized by sector and the 5 RCP global regions [13]. Importantly, the choice of harmonization method to date has been determined by individual experts and has generally been applied to all trajectories for a given class of emissions species.

Climate modeling efforts have continued to progress, demanding increased spatial and sectoral resolution from IAMs. Furthermore, a new generation of climate scenarios which combines aspects of both the RCPs and SSPs have been developed in order to incorporate both physical and socio-economic detail. In order to address the growing dimensionality of model outputs and support ongoing scenario generation and analysis efforts while still providing a consistent and scientifically rigorous harmonization procedure, an automated process for determining harmonization methods is preferred. The use of an automated, documented, and openly available harmonization mechanism additionally allows for full procedural reproducibility and for direct participation by additional modeling teams not involved in the original exercise.

The remainder of this paper describes the methodology and implementation of the harmonization software `aneris` [14], written in the Python programming language (detailed documentation is available online at `http://software.ene.iiasa.ac.at/aneris/`). Section 2 provides a detailed description of the underlying mathematical components of `aneris` as well as the procedural workflow. A case study of applying the automated harmonization mechanism on two example IAM scenarios, one with emissions growth and another with emissions mitigation, is presented in Section 3. Finally, the general effectiveness and potential future improvements on the automated methodology is discussed in Section 4.

Methodology & Implementation

The Conceptual Basis for Choosing Harmonization Methods

The goals of any scenario harmonization exercise are threefold: aligning model results in the harmonization year to a common historical data source, faithfully representing the original IAMs internal consistency between the driver of emissions (e.g. energy use) and emissions, and maintaining critical parameters from the original scenario design. Any harmonization method achieves the first goal by design. If the difference between the model base year and historical values are small, considering the second and third goals leads to a method choice that matches modeled drivers (e.g., a `ratio` method discussed in Section 2.2) and converges prior to the final model year. It preserves the relationship between IAM output and emissions inventory in the base year while also matching the original model output at some point in the modeled time period. It furthermore maintains the consistency of the model's usage of energy technology, volume of agricultural activities, and abatement options with harmonized emissions trajectory.

However, other concerns may lead to a better-informed choice than using a blanket method for all emissions trajectories. For example, emissions from LULUC are known to have high year-to-year variation, and therefore historical data may change drastically depending on the base year considered. In such a situation, a method that converges at a year past the modeled time period is a better choice in order to smooth out discrepancies between the historical data used to develop model and the new data source being used for harmonization.

Separately, if there are large discrepancies between the model results in the base year and the historic data used for harmonization, convergence methods can result in harmonized trajectories that do not faithfully represent the underlying drivers of emissions. Furthermore, if models report negative emissions, as is possible in scenarios designed to depict the deployment of climate mitigation policies with large CO_2 reductions and storage, then end-of-century emissions characteristics should be considered in order to faithfully match the design

parameters of the original scenarios, such as global mean temperature and other climate metrics.

Accordingly, we have developed a *decision tree* approach to harmonization method choice, discussed in Section 2.3, in order to balance each of these concerns and use cases in a robust, systematic, reproducible, and transparent manner.

Harmonization Methods

IAM emission results are provided along temporal (normally half decade or decade), spatial (i.e., model regions), emissions species, and sectoral dimensions. Each individual temporal trajectory, i.e., unique combinations of regions (r), species (g), and sectors (s), must be harmonized to the initial modeling period. Given a model trajectory, $m_{r,g,s}(t)$, historical values, $h_{r,g,s}(t)$, and model base year, t_i, a harmonized trajectory needs to be calculated. The *harmonization quality* of a trajectory, i.e., how well a given harmonization algorithm performs, depends on a number of factors. Of chief import is the faithful representation of the original unharmonized trajectory as well as the representation of negative trajectories (i.e., if a trajectory becomes negative, both the timing and total magnitude should be as close as possible) which are of critical importance for cumulative CO_2 calculations.

In previous studies [10, 12], two *families* of methods have been used: those that operate on the ratio of base year values (i.e., $\frac{h(t_i)}{m(t_i)}$) and those that operate on the offset of base year values (i.e., $h(t_i) - m(t_i)$). Both families of functions depend on a convergence factor, β, which scales linearly from 1 to 0 over $[t_i, t_f)$ and is shown in Equation 1. The use of the convergence factor implies that the ratio or offset applied in the base year (t_i) decays to the unharmonized model result (i.e., the convergence factor is 0) in the convergence year (t_f). In cases where the convergence factor is applied over the entire time horizon, the convergence year is taken to be $t_f = \infty$.

$$\beta(t, t_i, t_f) = \begin{cases} 1 - \frac{t - t_i}{t_f - t_i}, & \text{if } t < t_f \\ 0, & \text{otherwise} \end{cases} \tag{1}$$

A number methods are implemented in `aneris` including ratio-convergence shown in Equation 2, offset-convergence shown in Equation 3, and linear interpolation shown in Equation 4. In all equations the region, species, and sector indices have been dropped for clarity. Each equation is a function of time, model trajectory, historical trajectory, base year (t_i), and a convergence year (t_f), at which point the harmonized trajectory converges to the unharmonized trajectory. `aneris` provides a number of methods to choose from for each of the harmonization families. A summary of all available methods is provided in Table 1.

$$m^{rat}(t, m, h, t_i, t_f) = [\beta(t, t_i, t_f)(\frac{h(t_i)}{m(t_i)} - 1) + 1]m(t) \tag{2}$$

$$m^{off}(t, m, h, t_i, t_f) = \beta(t, t_i, t_f)(h(t_i) - m(t_i)) + m(t) \tag{3}$$

$$m^{int}(t, m, h, t_i, t_f) = \begin{cases} \beta(t, t_i, t_f)(h(t_i) - m(t_f)) + m(t_f), & \text{if } t < t_f \\ m(t), & \text{otherwise} \end{cases} \tag{4}$$

Table 1: All harmonization methods provided in `aneris`. A Convergence year of ∞ is provided for the `constant_ratio` and `constant_offset` methods are listed as $\beta = 1$ for all model years in both cases.

Method Name	Harmonization Family	Convergence Year
`constant_ratio`	ratio	$t_f = \infty$
`reduce_ratio_<year>`	ratio	$t_f =$`<year>`
`constant_offset`	offset	$t_f = \infty$
`reduce_offset_<year>`	offset	$t_f =$`<year>`
`linear_interpolate_<year>`	interpolation	$t_f =$`<year>`

Default Method Decision Tree

A *decision tree* approach has been implemented in `aneris` which provides a systematic and documented decision-making process to determine the preferred

harmonization algorithm. In order to provide reasonable *default* methods, the historical trajectory, unharmonized model trajectory, and relative difference between history and model values in the harmonization year are analyzed. The decision tree used in this analysis is a result of collaborative efforts between IAM teams and is shown graphically in Figure 1.

A number of characteristics impact the decision of which default method to select based on the effect of the characteristic on the potential harmonized trajectory. For example, it is rare but possible for a sector to have emissions reported in the historical data, but the model to report zero for the harmonization year, with non-zero future values. In such cases, an offset method is required as a ratio method would mask future emissions and erroneously harmonize the trajectory to zero.

In most cases, however, models do report values in the harmonization year. Figure 2 displays a number of example trajectories which highlight the possible issues resulting from harmonizing model results in different contexts. These trajectories do not correspond to specific model results; rather they serve as illustrative examples of the kinds of trajectories observed in practice. Panels `a` and `b` highlight examples where model results peak mid-century, behavior that is seen in a number of scenarios with general emissions mitigation effects, such as pollution controls applied by developing nations on transport and industry sectors. Panel `a` highlights a case where model base-year values and history are relative close whereas Panel `b` shows a situation where model values and history are relatively far apart. Panels `c` and `d` show similar model trajectories that peak mid-century but also have negative emissions. Models can report negative emissions for CO_2 in future scenarios with climate mitigation enacted via the deployment of carbon capture and storage technologies. Again, the relative difference with historical values differ between the panels to explore harmonization method choices in each situation.

When model and historical values are relatively close, a convergence method is chosen in order to be as representative as possible to the underlying unharmonized model results (Figure 2, Panel `a`). If values are not close, the constant ratio

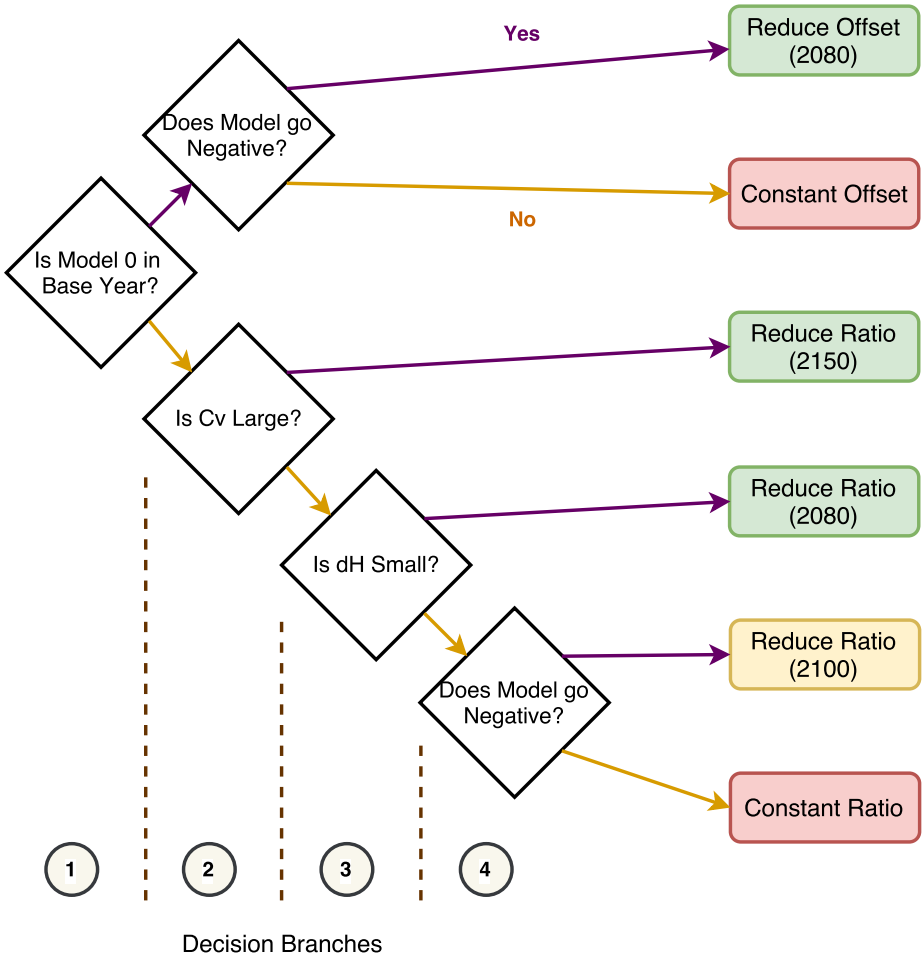

Figure 1: The default method decision tree used in the `aneris` software library. For all decisions, upper (purple) branches represent a "yes" response and lower (orange) branches represent a "no" response. The coefficient of variation, c_v, is defined in Equation 5, dH is defined as $\left|\frac{h(t_i)-m(t_i)}{h(t_i)}\right|$, and decision-making thresholds for c_v and dH are described in the main text. Where present, convergence years of default methods are provided below the method name in parentheses. Convergence years are chosen in order to balance the three harmonization goals discussed in Section 2.1. Methods labeled in *green* are likely to closely match unharmonized results, methods in *yellow* will likely somewhat match unharmonized results, and methods in *red* can be expected to have a large relative difference between harmonized and unharmonized results.

method is chosen in order to provide reasonable trajectories that still incorporate modeled effects (Figure 2, Panel b).

If a model provides a trajectory that transitions from positive to negative emissions and base year results are similar, then a convergence method is used in order to guarantee capture of this transition in a representative fashion (Figure 2, Panel c). If the discrepancy in base year results is large, it is possible for a negative trajectory to be inappropriately harmonized to a positive, but decreasing, trajectory. As such, the constant ratio method is chosen (Figure 2, Panel d).

Temporal variability of the historical trajectory is also an important characteristic when considering the choice of harmonization method. Emissions from forest and grassland fires, for example, vary from year to year due to a combination of meteorological conditions and anthropogenic drivers. Land use emissions in many IAMs are modeled using average emission factors and do not capture conditions in a specific year. A longer convergence horizon is thus desired in order to incorporate highly variable historical data with modeled results as is consistency in harmonization method because the effects are modeled similarly across regions and species. In order to detect emissions with a high amount of variation, a measure of the coefficient of variation, c_v, of the first derivative of the historical trajectory is calculated using the standard deviation, σ, and the mean, μ, as shown in Equation 5. For a single realization of c_v, the first derivative information of the entire historical time period is utilized.

$$c_v = \frac{\sigma(h'(t))}{\mu(h'(t))} \tag{5}$$

The value of c_v is then tested against a threshold, τ_{c_v}. To determine this threshold, an analysis of the recent CEDS and LULUC historical data has been performed. Figure 3 shows the distribution of LULUC c_vs and non-LULUC c_vs as determined for historical data aggregated to the model regions of 5 different IAMs involved in the SSP process: AIM-CGE [15], IMAGE[16], GCAM4[17], MESSAGE-GLOBIOM[18, 19], and REMIND-MAGPIE[20], each

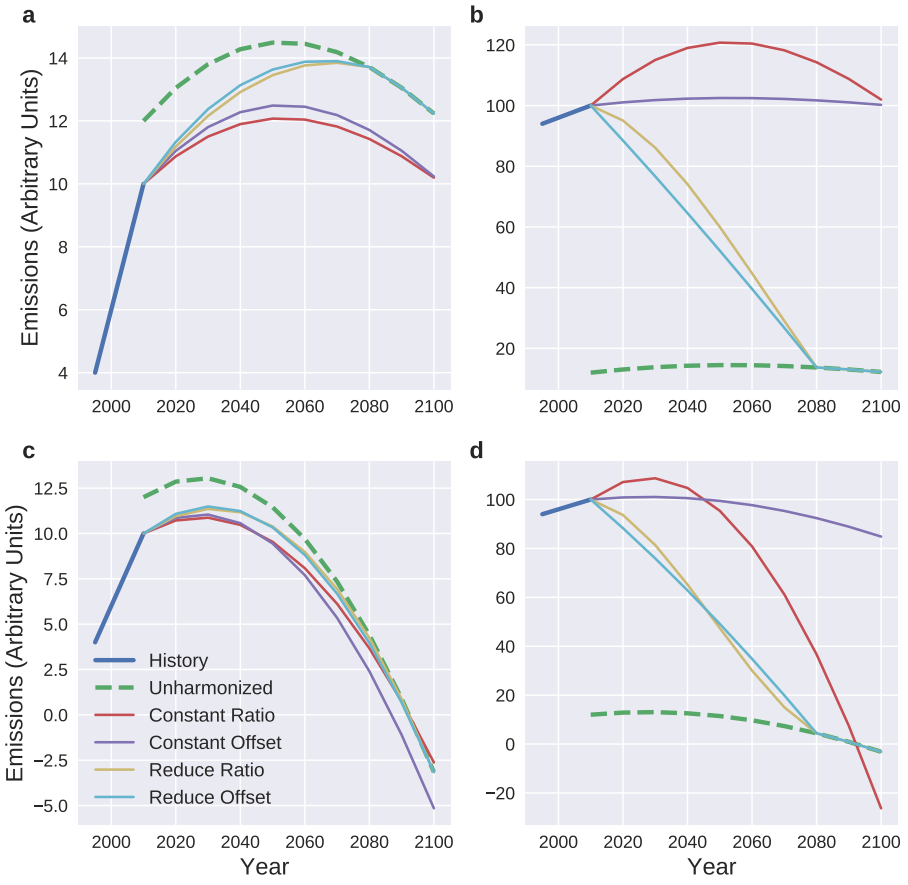

Figure 2: We present here a number of illustrative examples of the effect of different harmonization routines on model trajectories under "normal" circumstances (Panel `a`), when there is a large difference between historical and model values in the harmonization year (Panels `b` and `d`), and when model trajectories result in negative emissions by the end of the modeling time horizon (Panels `c` and `d`). Identical model trajectories are used in each row (Panels `a`, `b`; `c`, `d`). In each column, historical values are increased in the base year by an order of magnitude (from 10 to 100). In each Panel, a subset of the potential routines provide a better harmonization quality than others as described in the text.

of which have varying definitions of native model regions comprising different collections of countries. Therefore, each data point comprising Figure 3 represents a realization of c_v for a single combination of native model region, sector, and emissions species[2]. A threshold value of $\tau_{c_v} = 20$ has been chosen based on these observations as it optimally divides the two distributions. Importantly, tails of the LULUC and non-LULUC overlap, thus there are both false positives (7% of non-LULUC trajectories) and false negatives (10% of LULUC trajectories). However, as any regional definition is model dependent and thus any regional aggregation is possible an automated detection mechanism is necessary.

Finally, the default harmonization decisions depend on the relative difference between the historic and model values in the harmonization time period. In order to investigate the possible values that these relative differences can take, the IAM values used in the SSP and (ongoing) CMIP6 inter-comparison exercises are used. A distribution of these differences for all models in the study is presented in Figure 4. Given the available data, a threshold value of $\tau_{dH} = 50\%$ was chosen to be used as a default in `aneris`.

`aneris` Python Implementation and Workflow

We herein present `aneris`' Python implementation and conceptual design.. The library is composed of a number of utilities as well as three primary components: the `HarmonizationDriver`, `Harmonizer`, and data processing routines shown in red, green, and blue, respectively in Figures 5 and 6.

The `HarmonizationDriver` is an object designed to interface with user-provided data and configuration files. Input data (i.e., unharmonized model results) is assumed to be an Excel file in the standard data format within the IAM community, i.e., with `Model`, `Scenario`, `Region`, `Variable`, and `Unit` columns in addition to columns representing each modeled time period. It is responsible for down-selecting data into separate datasets for each model and scenario, invoking

[2] A full listing of all sectors and species is presented in the case-study discussion in Section 3, Table 3

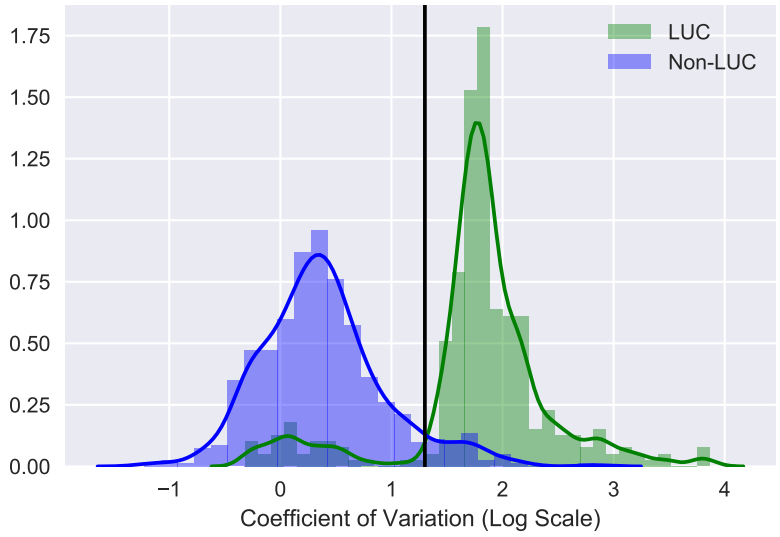

Figure 3: The distribution of c_v values for LULUC and non-LULUC historical trajectories is shown. CEDS historical data [8] is used for non-LULUC data and [9] is used for LULUC data. All historical data has been aggregated from their native spatial resolution (i.e., individual countries) to IAM model regional definitions (i.e., collections of countries), and all gas species included in the historical data sets are included in the analysis. The solid black line indicates the threshold value, τ_{c_v}, used by default in `aneris`.

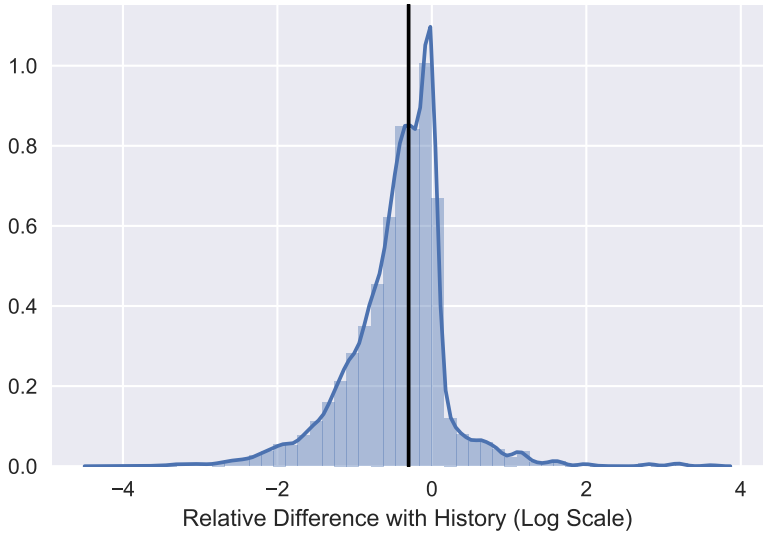

Figure 4: The distribution of relative differences between model and historical values in the harmonization year is shown. The solid black line indicates the 50% threshold value, τ_{dH}, used by default in `aneris`.

the harmonization process on each dataset, and recompiling the results. The `HarmonizationDriver` acts the primary interface for high-level users as shown by the usage of the `driver` object in Listing 1. Furthermore, a Command Line Interface (CLI) is provided to allow users to more easily incorporate the harmonization process in scripted workflows (Listing 2, Figure 5).

```
from aneris.tutorial import load_data
model, hist, driver = load_data()
for scenario in driver.scenarios():
    driver.harmonize(scenario)
harmonized, metadata = driver.harmonized_results()
```

Listing 1: High-level user interaction with the `HarmonizationDriver` taken from the online tutorial

```
$ aneris -h
usage: aneris [-h] [--history HISTORY] [--regions REGIONS] [--rc RC]
              [--output_path OUTPUT_PATH] [--output_prefix OUTPUT_PREFIX]
              input_file

    Harmonize historical trajectories to data in the IAM template format.

    Example usage:

    aneris input.xlsx --history history.csv --regions regions.csv

positional arguments:
  input_file            Input data file.

optional arguments:
  -h, --help            show this help message and exit
  --history HISTORY     Historical emissions in the base year.
  --regions REGIONS     Mapping of country iso-codes to native regions.
  --rc RC               Runcontrol YAML file (see
                        http://software.ene.iiasa.ac.at/aneris/config.html for
                        examples).
  --output_path OUTPUT_PATH
                        Path to use for output file names.
  --output_prefix OUTPUT_PREFIX
                        Prefix to use for output file names.
```

Listing 2: The CLI help provided by the `aneris` package.

The `Harmonizer` is a class whose task is to harmonize model value trajectories given historical data and possible user method *overrides*, i.e., non-default methods (described further in Section 2.5). It is used by the `HarmonizationDriver`;

however it is also available to the user as a first-class object. The `Harmonizer` requires that input data conform to the `aneris` calculation data format, which explicitly separates the emissions species from the sector contributing the emissions (these are combined in the single `Variable` column in the standard IAM format). Because the `Harmonizer` is designed to operate on a single instance of a model and scenario, the canonical data format includes `region`, `sector`, `gas`, and `units` columns without extraneous meta-data columns for the model and scenario. Once configured with appropriate input data (model and history) as well as potential method overrides, the `Harmonizer`'s `harmonize()` method can be invoked which returns a `pandas.DataFrame` of harmonized data. The object can additionally be queried directly as to its `default_methods()`, `methods()` (i.e., methods used with overrides), and `metadata()` (i.e., methods used with all branching information along each path in the decision tree).

There are also a variety of tools and utilities provided to users and also used by the `HarmonizationDriver` in order to process both input and output data. These include an `EmissionsAggregator` class and related routines used to generate sectoral emissions totals, generate regional totals, and combine historical emissions to native model regions (where historical data is defined at a higher spatial resolution than a model; see, e.g., Figure 7). A `FormatTranslator` class is also provided which defines an interface for translating `pandas.DataFrame`s between the IAM format expected for input and output data and the calculation format used by `aneris`' `Harmonizer`.

The full harmonization workflow, outlined in Figure 6, begins by cleaning input data. Cleaning operations include adding model trajectories with 0 values where a sector/emission combination exists in the historical data set but are not provided by the model input and detecting any issues that would cause the harmonization process to fail. The methods used to harmonize the data are then determined and the harmonization process is executed. Upon completion of the harmonization process, spatial aggregation to common analysis regions is performed. For example, the 5-region aggregation developed in the RCPs [13] process is commonly used in the IAM community and is shown in Figure

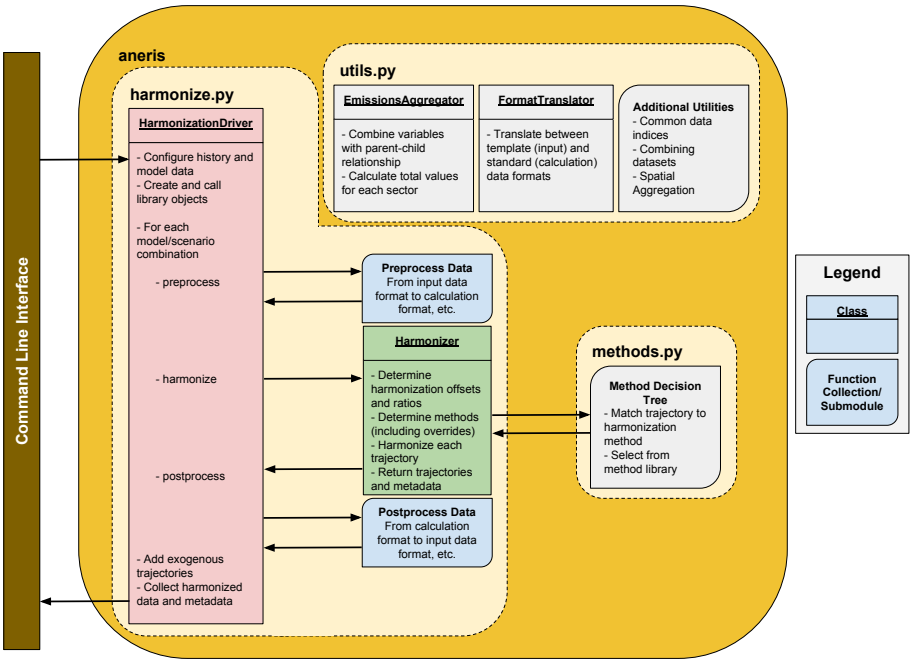

Figure 5: The various objects and their relation to one another in the `aneris` code base as well as a short description of their scope of concern.

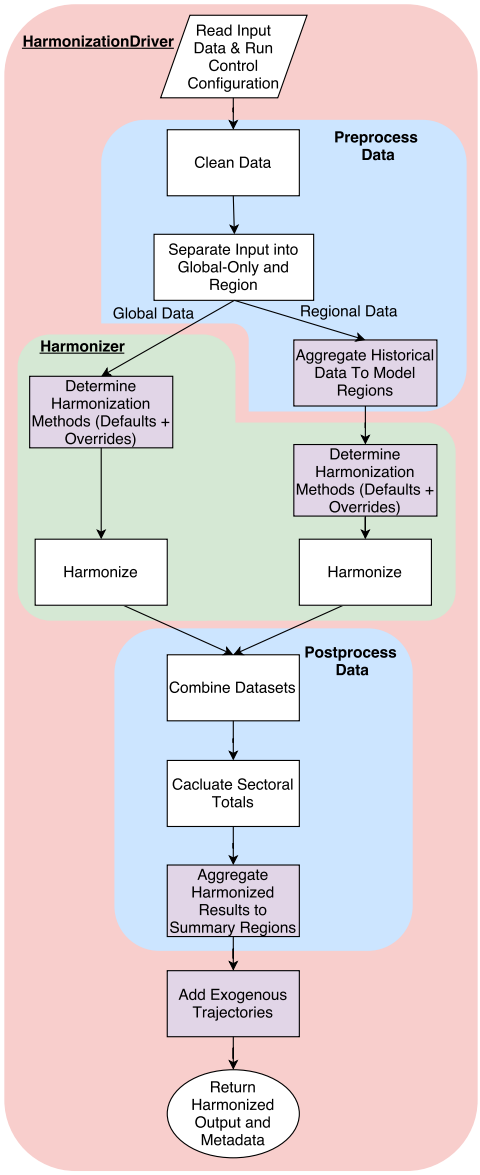

Figure 6: The full harmonization process as executed by `aneris` for a single instance of a model and scenario. Operations that can be configured with user-based input configurations are shown in purple. Operations governed by the `HarmonizationDriver` are shown in red. Data processing operations are shown in blue. The core harmonization process, governed by the `Harmonizer` is shown in green.

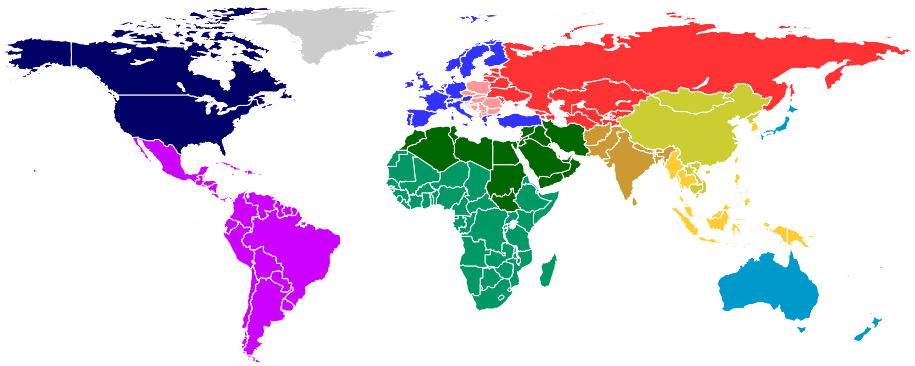

Figure 7: The 5 regions used in the RCPs with their MESSAGE-GLOBIOM 11-region constituents: Asia (Centrally-planned Asia and China (CPA), South Asia (SAS), Other Pacific Asia (PAS)) [yellows], Latin America and the Caribbean (LAM) [magenta], Africa and the Middle East (Middle East and North Africa (MEA) and Sub-Saharan Africa (AFR)) [greens], the OECD (North America (NAM), Western Europe (WEU), and Pacific OECD (PAO)) [blues], and the Reforming Economies (Central and Eastern Europe (EEU) and Former Soviet Union (FSU)) [reds].

7. Finally, any exogenous trajectories the user provides are added. Exogenous trajectories are normally provided for unmodeled gases with well-accepted scenario trajectories, e.g., chlorofluorocarbons provided by the World Meteorological Organization (WMO) [21]. Upon completion, the harmonized trajectories and meta data regarding the harmonization process are returned. A description of all returned meta data is provided in Table 2.

User-Defined Override Methods

Users are able to control the harmonization process via a number of options (with examples provided online). The primary mechanism by which users control the process is by providing *override* methods for any combination of region and variable (i.e., sector and gas species). In practice, it may be possible that not all default methods chosen will provide robust harmonized trajectories, especially if there is a significant difference between historical and model values in the harmonization year, if there is significant upward or downward movement in

Table 2: Meta data provided by the `aneris` harmonization routine. This meta data is provided for every combination of region, sector, and emissions species.

Column	**Description**
method	The harmonization method used.
default	The default harmonization method as determined by the default decision tree.
override	The method provided as an override (if any).
offset	The offset value between history and model in the harmonization year.
ratio	The ratio value between history and model in the harmonization year.
cov	The coefficient of variation value of the historical trajectory.
unharmonized	The unharmonized value in the harmonization year.
history	The historical value in the harmonization year.
harmonized	The resulting harmonized value in the harmonization year.

the model trajectory, or if there are known discrepancies in sectoral definition between the IAM and historical data source. In such cases, users can override default methods with their method of choice and both the default method and override is reported in the resulting metadata.

In order to help identify cases where overrides may be needed, harmonization *diagnostics* are provided which report the relative difference between harmonized and unharmonized trajectories at their mid and end-points when these values exceed specified thresholds. The diagnostic reporting thresholds are configurable by the user, but defaults of 400% and 200%, respectively, are provided based on experiences of the authors' use of `aneris` to date.

Case Study: Harmonizing Results from a Global IAM

In order to show a representative cross section of the performance of the `aneris` harmonization procedure, we focus on the harmonization of results of the IAM MESSAGE-GLOBIOM [18, 19]. Harmonization results for two scenarios from the SSP scenario library[3] are presented here. We use the SSP2-reference[18, 22], or "middle of the road", scenario (referred to as SSP2-Ref) as an example because MESSAGE-GLOBIOM is the marker scenario[4] for this SSP. This SSP2 scenario lies between two RCPs, 6 and 8.5, with a radiative forcing[5] level of approximately 6.5 Wm^{-2}. We additionally present the results for the SSP2-based mitigation scenario leading to a radiative forcing of 4.5 Wm^{-2} (referred to as SSP2-4.5). The SSP2-45 scenario is chosen because mitigation

[3] We refer the reader to the broad literature discussing the SSPs, e.g., [2, 3, 4, 6] for a more in depth discussion of the scenario architecture and design. Model results for various SSP scenarios are available online at `https://tntcat.iiasa.ac.at/SspDb`

[4] The "marker" scenario concept is used to designate the archetype scenario used as a reference within each SSP scenario family. See [2] and [4] for a more lengthy description.

[5] Radiative forcing in this context is the energy imbalance at the top of the atmosphere caused by anthropogenic influences relative to a pre-industrial reference point. Higher radiative forcing leads to larger global changes, such as surface temperature. We refer the reader to [23] for a more detailed discussion.

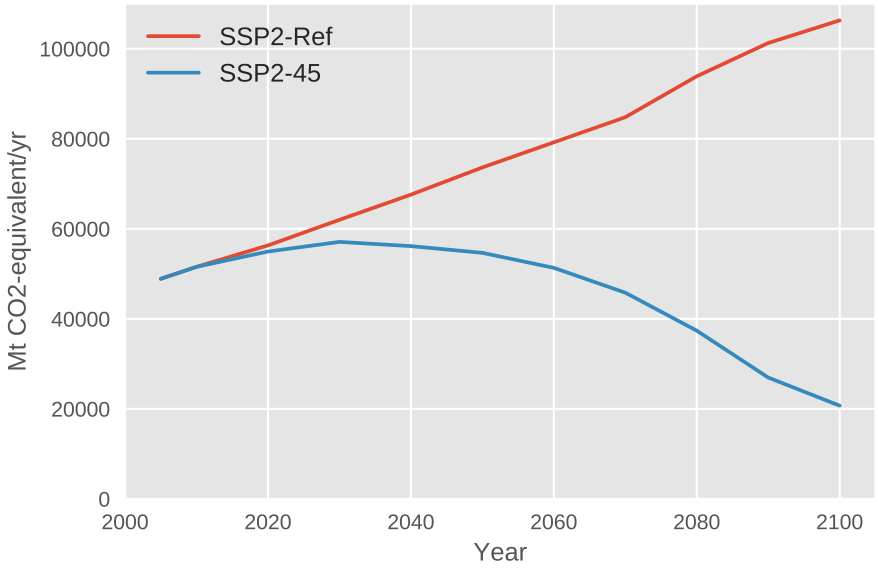

Figure 8: Unharmonized global Kyoto gas emissions for SSP2-Ref, a scenario with generally increasing global emissions trends, and SSP2-45, a scenario with generally decreasing global emissions trends.

technologies and policies are enacted causing a general reduction in pollutants and GHGs, including (eventual) negative CO_2 emissions in some regions and sectors due to carbon capture and sequestration and afforestation. A scenario in which negative emissions play a role in mitigation strategies is particularly important because of the sensitivity of key indicators, such as end-of-century radiative forcing (which is used to estimate mean global temperature response), to the timing and magnitude of net-zero and total negative CO_2 emissions. Therefore, these two scenarios represent two contrasting cases in the use of a harmonization approach and thus provide a case study as to its general applicability. Figure 8 shows the different trends of Kyoto Gases, a measure of aggregate GHG emissions, in each scenarios.

MESSAGE-GLOBIOM includes a representation of 11 distinct regions which can be mapped directly to the 5-region definition used in the RCPs (Figure 7);

harmonization is performed directly on the native regional spatial resolution. Historical data is taken from previously described LULUC and anthropogenic sources, which comprise 10 separate pollutant and GHG species and 12 sectors shown in Table 3. A total of 970 distinct trajectories[6] were harmonized for each scenario, and therefore 1940 trajectories were harmonized in total for these two illustrative scenarios. NO_x generated from the Energy sector provides an example of an emissions species and sector in which all regions were satisfactorily harmonized with the default methods. Figure 9 shows the results of harmonization in Asia, and Table 4 describes the parameters that underlie the choice of method for each harmonized trajectory. Importantly, the default methods provide regional trajectories for both the reference and mitigation scenarios that match the general unharmonized model behavior and also result in global aggregated emissions that are similar to the unharmonized trajectory.

The harmonization of emissions pathways is performed in order to accurately represent new or updated data sets of historical emissions inventories while also maintaining consistency with the original, unharmonized pathway. As such, when the default methods as provided by the harmonization procedure distort or otherwise sufficiently misrepresent the underlying unharmonized results, an override method is required to be provided for the trajectory of the region, sector, and species in question. Of the 970 trajectories, approximately 10% were reported as a diagnostic (see Section 2.4) of which 3.5% required the use of harmonization overrides after an initial investigation; thus, 96.5% of all trajectories were satisfactorily harmonized using the default methods. The trajectories that required overrides clustered into two classifications: regional trajectories whose *magnitude* was overly distorted and regional trajectories whose *shape* was overly distorted.

Figure 10 presents a case in which the magnitude of a trajectory is distorted. A large discrepancy (∼300% relative difference) is observed in the harmonization

[6]Table 3 compiles 24 global trajectories and 86 regional trajectories. Therefore, with 11 model regions, 970 total trajectories are harmonized.

Table 3: Harmonized Species and Sectors

Emissions Species	**Sectors**
Black Carbon (BC)	Agricultural Waste Burning[c]
Hexafluoroethane (C_2F_6) [a]	Agriculture[c]
Tetrafluoromethane (CF_4) [a]	Aircraft [b]
Methane (CH_4)	Energy Sector
Carbon Dioxide (CO_2) [c]	Forest Burning[c]
Carbon Monoxide (CO)	Grassland Burning[c]
Hydrofluorocarbons (HFCs) [a]	Industrial Sector
Nitrous Oxide (N_2O) [a]	International Shipping[b]
Ammonia (NH_3)	Residential Commercial Other
Nitrogen Oxides (NO_x)	Solvents Production and Application
Organic Carbon (OC)	Transportation Sector
Sulfur Hexafluoride (SF_6) [a]	Waste
Sulfur Oxides (SO_x)	
Volatile Organic Compounds (VOCs)	

[a] Global total trajectories are harmonized due to lack of detailed historical data.

[b] Global sectoral trajectories are harmonized due to lack of detailed historical data.

[c] A global trajectory for land-use CO_2 is used; non-land-use sectors are harmonized for each model region.

Table 4: Key Parameters for Deciding Harmonization Methods for NO_x Emissions in the Energy Sector in Asia

Region	**dH**	**c_v**	**Decision Tree Traversal (Branch and Direction)**	**Default Method Chosen**
CPA	0.35	2.26	1 (no), 2 (no), 3 (yes)	reduce_ratio_2080
PAS	0.14	1.24	1 (no), 2 (no), 3 (yes)	reduce_ratio_2080
SAS	0.56	0.58	1 (no), 2 (no), 3 (no), 4 (no)	constant_ratio

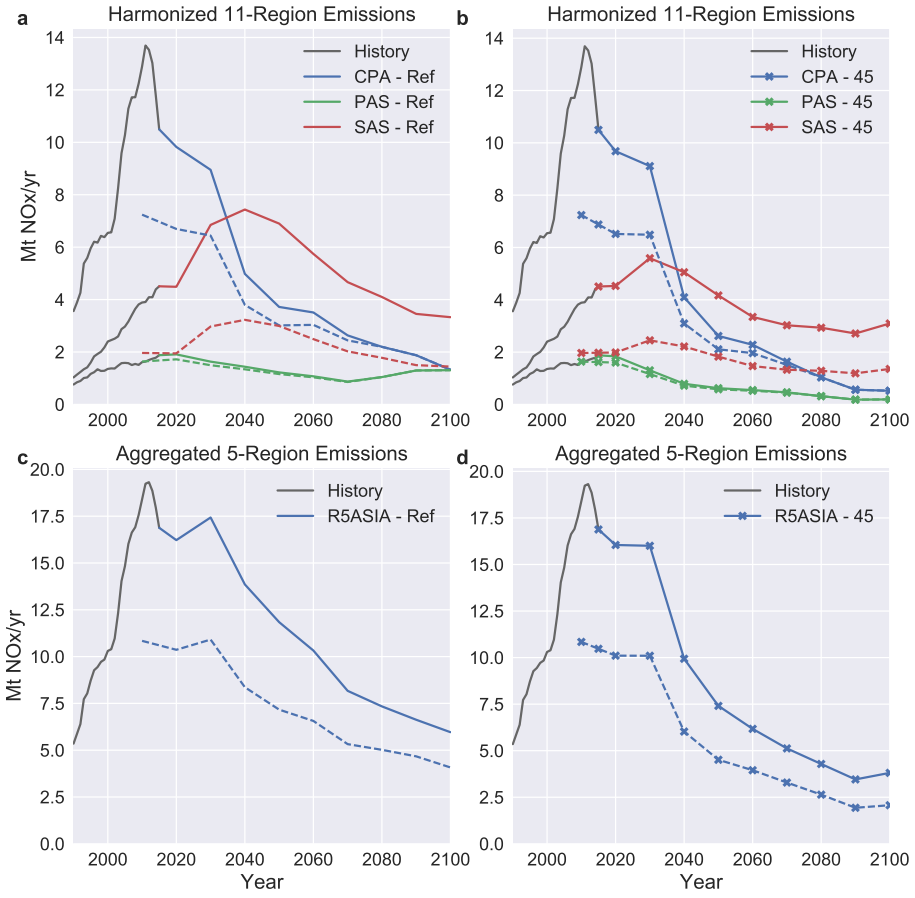

Figure 9: NO_x Energy Sector harmonized (solid lines) and unharmonized (dashed lines) trajectories for SSP2 and SSP2-45 with historical trajectories (grey lines) are presented. The SSP2 reference scenario is shown in Panels **a** and **c**; the SSP-45 scenario is denoted with "x" markers in Panels **b** and **d**. The upper panels show the results for endogenously modeled and harmonized regions in Asia while the lower panels display the aggregate region results.

year for carbon monoxide (CO) emissions in the industrial sector specifically for the SAS and AFR regions. Furthermore, emissions in both regions see relatively large expansion or contraction, depending on the scenario; therefore, both regions are candidates for choosing harmonization method overrides. The default method chosen in both cases (`constant_ratio`) maintains model trends for the region; however, overall model results are distorted as can be seen in both the regional and global panels in Figure 10. By applying `constant_offset` overrides, the regional trends and magnitudes are maintained. The use of harmonization overrides also ameliorates issues seen in the harmonized global trajectory of industrial CO (Figure 10, Panel **c**). Not only does the global trajectory with overrides more closely match the original unharmonized model behavior and magnitude of emissions, but the relative importance of the underlying regional trajectories is also maintained.

In certain circumstances, the application of the default harmonization methods can affect not only the magnitude but also the shape of regional trajectories. Figure 11 shows an example case of emissions trajectories for ammonia (NH_3) from the agriculture sector. Again, the SAS region shows a large discrepancy in the harmonization year (>150% in this case). The resulting trajectory harmonized with the default method (`constant_ratio`) provides a large increase after 2080 in the SSP2 reference scenario. Notably, the SSP2-45 scenario is not affected to the same degree. While this distortion changes the magnitude of the SAS trajectory, it largely affects the post-2080 shape of the global trajectory (Figure 11, Panel **b**) as well as the relative regional contributions to the global aggregate trajectory. For example, in the original model result, SAS NH_3 agricultural emissions contribute ∼30% of total global emissions, whereas in the harmonized case with default methods, SAS comprises ∼50% of global emissions by 2100. By using a `constant_offset` method as an override, this distortion is addressed and more accurately reflects unharmonized results in the SAS region, the relative importance between regions, and global results for agricultural ammonia emissions, each of which contributes to a better harmonization quality for the harmonized SAS trajectory. The harmonized emissions using overrides result in

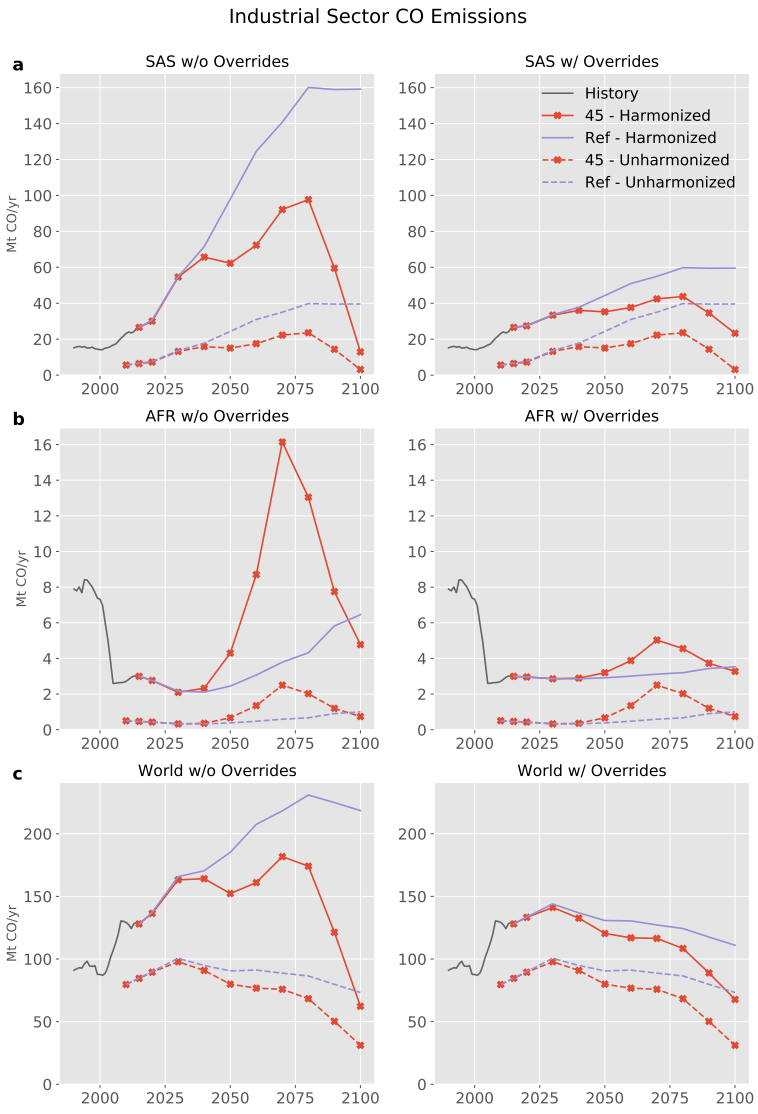

Figure 10: CO Industrial Sector harmonized (without markers) and unharmonized (with markers) emissions are presented for SSP2 (purple lines) and SSP2-45 (red lines) scenarios. The left column shows the default harmonization and the right column shows harmonization with overrides. Panel **a** shows trajectories for the SAS region while panels **b** and **c** show trajectories for the AFR region and (total) global emissions, respectively. Notably, the SAS and AFR regional trajectories are distorted when the default methods are used due to the harmonization-year difference between history and model results in both scenarios. The distortion is large enough to affect global results, as shown in Panel **c**. The use of overrides (right column) results in better consistency with the unharmonized model scenario at the regional and global levels.

a contribution of ∼32% of total global emissions by the SAS region which aligns closely with the unharmonized model results.

We investigate the aggregate effect of harmonization with all necessary override methods on total anthropogenic radiative forcing projections with the simple carbon-cycle and climate model, MAGICC[7] [24, 25], for each harmonized and unharmonized scenario respectively as shown in Figure 12. We find that the change due to harmonization is small, ranging between 1 and 2.5% over the modeled time period. Relative near-term differences persist in the mitigation case (SSP-4.5) because differences in near-term emissions define to a larger degree the longer-term forcing outcome due to the cumulative nature of long-lived climate forcers like CO_2 . The resulting difference in forcing in 2100 is 0.04 $\frac{\mathrm{W}}{\mathrm{m}^2}$ for SSP2-4.5 and 0.01 $\frac{\mathrm{W}}{\mathrm{m}^2}$ for SSP2-Ref, both of which are well within acceptable tolerances (e.g., 0.75 $\frac{\mathrm{W}}{\mathrm{m}^2}$ defined for ScenarioMIP [6]). Thus harmonization is considered to have a negligible effect on key long-term climate indicators.

Discussion & Future Work

This work presented a novel methodology and Python implementation of automated emissions harmonization for IAMs, `aneris`. An in-depth explanation of the processes and methods for determining the use of harmonization methods was provided in Section 2. `aneris` was able to satisfactorily harmonize over 96% of the 1940 individual trajectories that were analyzed in Section 3. Of the remaining trajectories, harmonization method overrides were applied, and discussion was provided detailing why overrides were deemed necessary.

The automated approach drastically reduces the need for expert opinion in determining harmonization methods for each individual combination of model region, sector, and emissions species while still providing a justifiable explanation

[7]MAGICC is a reduced complexity climate model which incorporates future trajectories of forcing agents (i.e., emissions) to estimate future radiative forcing and mean global temperature response. We refer the reader to the MAGICC wiki (available online: `http://wiki.magicc.org`) for a more in-depth description.

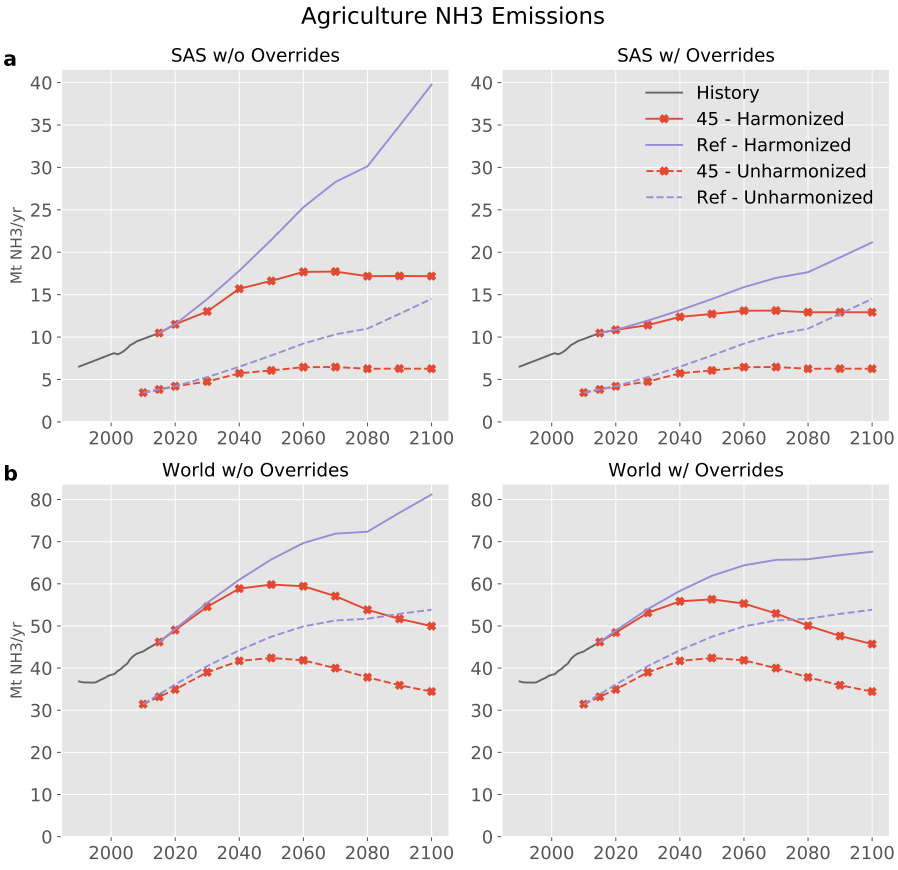

Figure 11: NH_3 agricultural harmonized and unharmonized emissions are presented for SSP2 and SSP2-45 scenarios. Panel **a** shows harmonized and overridden-harmonized (respectively) trajectories for the SAS region, and panel **b** shows the global total trajectory. In this case, the SAS trajectory again shows not only a magnitude distortion, but also a shape distortion at the tail of the trajectory. Additionally, global trajectories are greatly affected by the harmonization method choice (there is ∼20% relative difference between trajectories in the reference scenario in 2100). Override methods have been applied to correct the distortion.

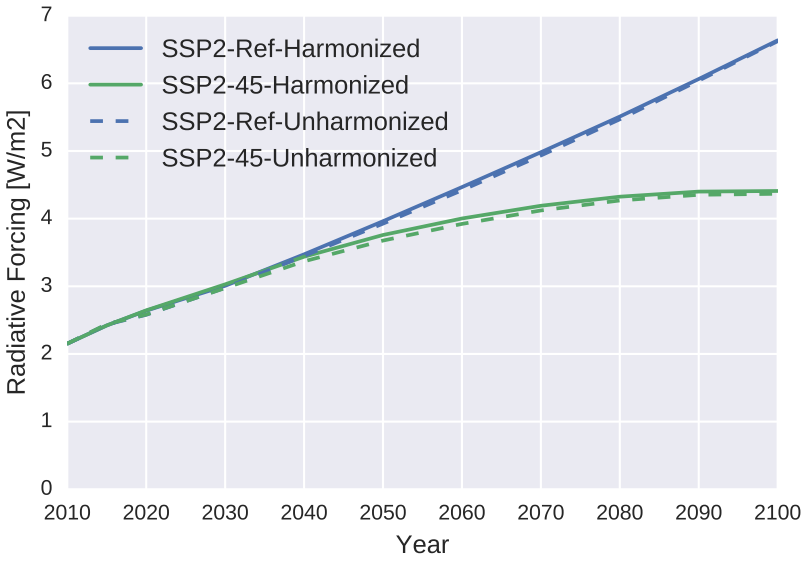

Figure 12: The results of the simple climate model, MAGICC6, forced with the SSP2-Ref (blue) and SSP2-4.5 (green) harmonized and unharmonized scenarios is presented. The radiative forcing trajectories of harmonized and unharmonized scenarios are shown in solid lines and dashed lines, respectively.

for each automated choice of harmonization method based on both the historical and future emissions trajectories. Furthermore, the automated approach should continue to scale well as models become more detailed in both the regional and sectoral dimensions. Finally, expert opinion is still allowed to trump the automated method as determined by the algorithm via method overrides; however, these cases are clearly documented via the meta data provided as an output of `aneris` and thus can be individually explained. This provides not only transparency and reproducibility, but also scientific integrity in the choice of harmonization methods.

The use of an open-source, automated harmonization process also provides benefits to the wider climate science and IAM communities. By providing a standard mechanism for harmonization, the IAM community can directly provide input into the harmonization algorithms and rules for their default selection. Additionally, modeling teams are easily capable of executing identical harmonization procedures in order to participate in ongoing and further iterations of intercomparison exercises and analysis. Future scenario analyses can also utilize this common harmonization approach such that they are consistent with prior efforts.

There are a variety of avenues for future improvement of both the `aneris` software and underlying methodology. As with any software project, additional users will provide use cases for more robust handling of input/output issues and corner cases. Further configuration parameters can also be added in the future in order to provide overrides for all gas species in a given sector or region. Perhaps the most fruitful investigation will involve further refinement of the default decision tree introduced in Section 2. A key aspect missing from the decision tree is input from models regarding whether missing sources or activity levels are the likely cause of a harmonization year discrepancy (suggesting the use of an offset method) or instead a significant difference in emissions factors (suggesting the use of a ratio method) [12].

This work provides a new direction and framework which the IAM and climate science communities can build upon in order to reduce the necessity

of consistent expert opinion and increase transparency and reproducibility of harmonization exercises. Furthermore, it provides an open-source, tested, and documented software library which can be used and improved upon by these communities. Both of these are clear steps in a positive direction for future climate and integrated assessment modeling exercises.

Acknowledgments

The authors would like to acknowledge a number of colleagues who helped contribute both discussion and feedback regarding this work including Drs. Elmar Kriegler, Gunnar Luderer, and Joeri Rogelj. This project has received funding from the European Unions Horizon 2020 research and innovation programme under grant agreement No 641816. The authors further wish to thank the Global Environment Facility for their generous financial support.

Acronyms

AerChemMIP Aerosol Chemistry Model Intercomparison Project. 4

AFR Sub-Saharan Africa. 22, 29, 30

CEDS Community Emissions Data System. 5, 12, 15

CLI Command Line Interface. 17, 18

CMIP6 Coupled Model Intercomparison Project (Phase 6). 4, 5, 14

CPA Centrally-planned Asia and China. 22, 27

EEU Central and Eastern Europe. 22

ESM Earth System Model. 4

FSU Former Soviet Union. 22

GHG Greenhouse Gas. 4, 5, 25, 26

IAM Integrated Assessment Model. 4–8, 10, 12, 14, 15, 19, 24, 31, 34

LAM Latin America and the Caribbean. 22

LULUC Land-use and Land-use Change. 5, 7, 12, 14, 15, 26

MEA Middle East and North Africa. 22

NAM North America. 22

PAO Pacific OECD. 22

PAS Other Pacific Asia. 22, 27

RCP Representative Concentration Pathway. 6, 19, 22, 24

SAS South Asia. 22, 27, 29–32

ScenarioMIP Scenario Model Intercomparison Project. 4, 31

SRES Special Report on Emissions Scenarios. 5

SSP Shared Socioeconomic Pathway. 4–6, 12, 14, 24

WEU Western Europe. 22

WMO World Meteorological Organization. 22

References

[1] V. Krey, Global energy-climate scenarios and models: a review, Wiley Interdisciplinary Reviews: Energy and Environment 3 (4) (2014) 363–383. doi:10.1002/wene.98.
URL http://onlinelibrary.wiley.com/doi/10.1002/wene.98/abstract

[2] K. Riahi, D. P. van Vuuren, E. Kriegler, J. Edmonds, B. C. ONeill, S. Fujimori, N. Bauer, K. Calvin, R. Dellink, O. Fricko, W. Lutz, A. Popp, J. C. Cuaresma, S. KC, M. Leimbach, L. Jiang, T. Kram, S. Rao, J. Emmerling, K. Ebi, T. Hasegawa, P. Havlik, F. Humpender, L. A. D. Silva, S. Smith, E. Stehfest, V. Bosetti, J. Eom, D. Gernaat, T. Masui, J. Rogelj, J. Strefler, L. Drouet, V. Krey, G. Luderer, M. Harmsen, K. Takahashi, L. Baumstark, J. C. Doelman, M. Kainuma, Z. Klimont, G. Marangoni, H. Lotze-Campen, M. Obersteiner, A. Tabeau, M. Tavoni, The shared socioeconomic pathways and their energy, land use, and greenhouse gas emissions implications: An overview, Global Environmental Change 42 (2017) 153 – 168. doi:https://doi.org/10.1016/j.gloenvcha.2016.05.009.
URL http://www.sciencedirect.com/science/article/pii/S0959378016300681

[3] B. C. ONeill, E. Kriegler, K. Riahi, K. L. Ebi, S. Hallegatte, T. R. Carter, R. Mathur, D. P. v. Vuuren, A new scenario framework for climate change research: the concept of shared socioeconomic pathways, Climatic Change 122 (3) (2013) 387–400. doi:10.1007/s10584-013-0905-2.
URL http://link.springer.com/article/10.1007/s10584-013-0905-2

[4] D. P. v. Vuuren, E. Kriegler, B. C. ONeill, K. L. Ebi, K. Riahi, T. R. Carter, J. Edmonds, S. Hallegatte, T. Kram, R. Mathur, H. Winkler, A new scenario framework for Climate Change Research: scenario matrix architecture, Climatic Change 122 (3) (2013) 373–386. doi:10.1007/s10584-013-0906-1.

URL http://link.springer.com/article/10.1007/s10584-013-0906-1

[5] V. Eyring, S. Bony, G. A. Meehl, C. A. Senior, B. Stevens, R. J. Stouffer, K. E. Taylor, Overview of the Coupled Model Intercomparison Project Phase 6 (CMIP6) experimental design and organization, Geosci. Model Dev. 9 (5) (2016) 1937–1958. doi:10.5194/gmd-9-1937-2016.
URL http://www.geosci-model-dev.net/9/1937/2016/

[6] B. C. O'Neill, C. Tebaldi, D. P. van Vuuren, V. Eyring, P. Friedlingstein, G. Hurtt, R. Knutti, E. Kriegler, J.-F. Lamarque, J. Lowe, others, The scenario model intercomparison project (scenariomip) for CMIP6, Geoscientific Model Development 9 (9) (2016) 3461.
URL http://search.proquest.com/openview/e2eae675069c0ff45c7f19861f7dfcca/1?pq-origsite=gscholar&cbl=105726

[7] W. J. Collins, J.-F. Lamarque, M. Schulz, O. Boucher, V. Eyring, M. I. Hegglin, A. Maycock, G. Myhre, M. Prather, D. Shindell, S. J. Smith, AerChemMIP: quantifying the effects of chemistry and aerosols in CMIP6, Geosci. Model Dev. 10 (2) (2017) 585–607. doi:10.5194/gmd-10-585-2017.
URL https://www.geosci-model-dev.net/10/585/2017/

[8] R. M. Hoesly, S. J. Smith, L. Feng, Z. Klimont, G. Janssens-Maenhout, T. Pitkanen, J. J. Seibert, L. Vu, R. J. Andres, R. M. Bolt, T. C. Bond, L. Dawidowski, N. Kholod, J.-I. Kurokawa, M. Li, L. Liu, Z. Lu, M. C. P. Moura, P. R. O'Rourke, Q. Zhang, Historical (17502014) anthropogenic emissions of reactive gases and aerosols from the Community Emissions Data System (CEDS), Geosci. Model Dev. 11 (1) (2018) 369–408. doi:10.5194/gmd-11-369-2018.
URL https://www.geosci-model-dev.net/11/369/2018/

[9] M. J. E. van Marle, S. Kloster, B. I. Magi, J. R. Marlon, A.-L. Daniau, R. D. Field, A. Arneth, M. Forrest, S. Hantson, N. M. Kehrwald, W. Knorr,

G. Lasslop, F. Li, S. Mangeon, C. Yue, J. W. Kaiser, G. R. van der Werf, Historic global biomass burning emissions for CMIP6 (BB4cmip) based on merging satellite observations with proxies and fire models (17502015), Geosci. Model Dev. 10 (9) (2017) 3329–3357. doi:10.5194/gmd-10-3329-2017.
URL https://www.geosci-model-dev.net/10/3329/2017/

[10] M. Meinshausen, S. J. Smith, K. Calvin, J. S. Daniel, M. L. T. Kainuma, J.-F. Lamarque, K. Matsumoto, S. A. Montzka, S. C. B. Raper, K. Riahi, A. Thomson, G. J. M. Velders, D. P. P. v. Vuuren, The RCP greenhouse gas concentrations and their extensions from 1765 to 2300, Climatic Change 109 (1-2) (2011) 213. doi:10.1007/s10584-011-0156-z.
URL https://link.springer.com/article/10.1007/s10584-011-0156-z

[11] N. Nakićenović, J. Alcamo, G. Davis, B. de Vries, J. Fenhann, S. Gaffin, K. Gregory, A. Grübler, T. Y. Jung, T. Kram, E. Lebre La Rovere, L. Michaelis, S. Mori, T. Morita, W. Pepper, H. Pitcher, L. Price, K. Riahi, A. Roehrl, H. H. Rogner, A. Sankovski, M. Schlesinger, P. Shukla, S. Smith, R. Swart, S. van Rooijen, N. Victor, Z. Dadi, IPCC Special Report on Emissions Scenarios (SRES), Cambridge University Press, UK, 2000.
URL http://www.ipcc.ch/ipccreports/sres/emission/index.php?idp=0

[12] J. Rogelj, W. Hare, C. Chen, M. Meinshausen, Discrepancies in historical emissions point to a wider 2020 gap between 2 C benchmarks and aggregated national mitigation pledges, Environmental Research Letters 6 (2) (2011) 024002. doi:10.1088/1748-9326/6/2/024002.
URL http://stacks.iop.org/1748-9326/6/i=2/a=024002

[13] D. P. v. Vuuren, J. Edmonds, M. Kainuma, K. Riahi, A. Thomson, K. Hibbard, G. C. Hurtt, T. Kram, V. Krey, J.-F. Lamarque, T. Masui, M. Meinshausen, N. Nakicenovic, S. J. Smith, S. K. Rose, The representative concentration pathways: an overview, Climatic Change 109 (1-2) (2011)

5–31. doi:10.1007/s10584-011-0148-z.
URL http://link.springer.com/article/10.1007/s10584-011-0148-z

[14] M. Gidden, aneris: Harmonization for Integrated Assessment Models (Jun. 2017). doi:10.5281/zenodo.802832.
URL https://doi.org/10.5281/zenodo.802832

[15] S. Fujimori, T. Hasegawa, T. Masui, K. Takahashi, D. S. Herran, H. Dai, Y. Hijioka, M. Kainuma, SSP3: AIM implementation of Shared Socioeconomic Pathways, Global Environmental Change 42 (2017) 268–283. doi:10.1016/j.gloenvcha.2016.06.009.
URL http://www.sciencedirect.com/science/article/pii/S0959378016300838

[16] D. P. van Vuuren, E. Stehfest, D. E. H. J. Gernaat, J. C. Doelman, M. van den Berg, M. Harmsen, H. S. de Boer, L. F. Bouwman, V. Daioglou, O. Y. Edelenbosch, B. Girod, T. Kram, L. Lassaletta, P. L. Lucas, H. van Meijl, C. Mller, B. J. van Ruijven, S. van der Sluis, A. Tabeau, Energy, land-use and greenhouse gas emissions trajectories under a green growth paradigm, Global Environmental Change 42 (2017) 237–250. doi:10.1016/j.gloenvcha.2016.05.008.
URL http://www.sciencedirect.com/science/article/pii/S095937801630067X

[17] K. Calvin, B. Bond-Lamberty, L. Clarke, J. Edmonds, J. Eom, C. Hartin, S. Kim, P. Kyle, R. Link, R. Moss, H. McJeon, P. Patel, S. Smith, S. Waldhoff, M. Wise, The SSP4: A world of deepening inequality, Global Environmental Change 42 (2017) 284–296. doi:10.1016/j.gloenvcha.2016.06.010.
URL http://www.sciencedirect.com/science/article/pii/S095937801630084X

[18] O. Fricko, P. Havlik, J. Rogelj, Z. Klimont, M. Gusti, N. Johnson,

P. Kolp, M. Strubegger, H. Valin, M. Amann, T. Ermolieva, N. Forsell, M. Herrero, C. Heyes, G. Kindermann, V. Krey, D. L. McCollum, M. Obersteiner, S. Pachauri, S. Rao, E. Schmid, W. Schoepp, K. Riahi, The marker quantification of the Shared Socioeconomic Pathway 2: A middle-of-the-road scenario for the 21st century, Global Environmental Change 42 (2017) 251–267. doi:10.1016/j.gloenvcha.2016.06.004.
URL http://www.sciencedirect.com/science/article/pii/S0959378016300784

[19] V. Krey, P. Havlik, O. Fricko, J. Zilliacus, M. Gidden, M. Strubegger, G. Kartasasmita, T. Ermolieva, N. Forsell, M. Gusti, N. Johnson, G. Kindermann, P. Kolp, D. L. McCollum, S. Pachauri, S. Rao, J. Rogelj, H. Valin, M. Obersteiner, K. Riahi, MESSAGE-GLOBIOM 1.0 Documentation, Tech. rep., International Institute for Applied Systems Analysis (IIASA) (2016).
URL http://data.ene.iiasa.ac.at/message-globiom/

[20] E. Kriegler, N. Bauer, A. Popp, F. Humpender, M. Leimbach, J. Strefler, L. Baumstark, B. L. Bodirsky, J. Hilaire, D. Klein, I. Mouratiadou, I. Weindl, C. Bertram, J.-P. Dietrich, G. Luderer, M. Pehl, R. Pietzcker, F. Piontek, H. Lotze-Campen, A. Biewald, M. Bonsch, A. Giannousakis, U. Kreidenweis, C. Mller, S. Rolinski, A. Schultes, J. Schwanitz, M. Stevanovic, K. Calvin, J. Emmerling, S. Fujimori, O. Edenhofer, Fossil-fueled development (SSP5): An energy and resource intensive scenario for the 21st century, Global Environmental Change 42 (2017) 297–315. doi:10.1016/j.gloenvcha.2016.05.015.
URL http://www.sciencedirect.com/science/article/pii/S0959378016300711

[21] A. R. Ravishankara, P. A. Newman, J. A. Pyle, A. N. Ajavon, et al., Scientific Assessment of Ozone Depletion: 2014, Tech. rep., Global Ozone Research and Monitoring Project, World Meteorological Organization, Geneva, Switzerland (2014).

[22] S. Rao, Z. Klimont, S. J. Smith, R. V. Dingenen, F. Dentener, L. Bouwman, K. Riahi, M. Amann, B. L. Bodirsky, D. P. van Vuuren, L. A. Reis, K. Calvin, L. Drouet, O. Fricko, S. Fujimori, D. Gernaat, P. Havlik, M. Harmsen, T. Hasegawa, C. Heyes, J. Hilaire, G. Luderer, T. Masui, E. Stehfest, J. Strefler, S. van der Sluis, M. Tavoni, Future air pollution in the shared socio-economic pathways, Global Environmental Change 42 (2017) 346 – 358. doi:https://doi.org/10.1016/j.gloenvcha.2016.05.012.
URL http://www.sciencedirect.com/science/article/pii/S0959378016300723

[23] IPCC, Climate Change 2013: The Physical Science Basis. Contribution of Working Group I to the Fifth Assessment Report of the Intergovernmental Panel on Climate Change, Cambridge University Press, Cambridge, United Kingdom and New York, NY, USA, 2013. doi:10.1017/CBO9781107415324.
URL www.climatechange2013.org

[24] M. Meinshausen, S. C. Raper, T. M. Wigley, Emulating coupled atmosphere-ocean and carbon cycle models with a simpler model, magicc6–part 1: Model description and calibration, Atmospheric Chemistry and Physics 11 (4) (2011) 1417–1456.

[25] M. Meinshausen, S. J. Smith, K. Calvin, J. S. Daniel, M. Kainuma, J. Lamarque, K. Matsumoto, S. Montzka, S. Raper, K. Riahi, et al., The rcp greenhouse gas concentrations and their extensions from 1765 to 2300, Climatic change 109 (1-2) (2011) 213.